ARTICLE

High Spatial Variability in Under-Ice Export Fluxes over the Chukchi Plateau in the Pacific Arctic Region

Catherine Lalande[1] · Jong-Kuk Moon[1] · Jinyoung Jung[1] · Eun Jin Yang[1]

Abstract

A large proportion of algal production and carbon export occurs after snowmelt and before ice melt in the Arctic Ocean. To determine the magnitude of under-ice export fluxes over the Chukchi Plateau (CP), a total of 25 sediment trap deployments were completed at two ice camps during the annual field survey of the Korean IBRV *Araon* in 2018: a first ice camp (CP1) conducted from August 17 to 19 and a second ice camp (CP2) conducted from August 20 to 22. Chlorophyll *a* (chl *a*) and particulate organic carbon (POC) fluxes were measured at 2, 5, 10 and 30 m under ice, and zooplankton collected in the sediment traps were enumerated and identified. Both chl *a* and POC fluxes were the highest at 5 m under ice at CP2, likely due to enhanced fluxes of the sea ice algae *Melosira arctica* and to a potential higher release of particulate matter from a thinner sea ice cover. Whereas *Calanus glacialis/marshallae* were dominant at all depths and both sites, the large numbers of individuals observed at 10 m at CP1 likely enhanced zooplankton grazing pressure at that site, further contributing to the high spatial variability in under-ice export fluxes. Overall, under-ice fluxes obtained in August 2018 highlighted the importance of *M. arctica* aggregates as a source of carbon for pelagic consumers and for carbon export during summer over the Chukchi Plateau.

Keywords Arctic Ocean · Carbon export · Chukchi Plateau · Sea ice algae · Sediment trap

1 Introduction

In the Arctic Ocean, high seasonal variation in sunlight and ice conditions regulates primary production both within and under the sea ice in the upper water column (Fortier et al. 2002; Leu et al. 2015). Sea ice algae growth starts at the bottom of the ice when incident solar radiation is sufficient, and ends with their release into the water column during snow and ice melt (Cota 1991; Juul-Pedersen et al. 2008; Campbell et al. 2015). Concurrently, the increased irradiance and the haline stratification resulting from snow and sea ice melt rapidly trigger the onset of a pelagic algal bloom, which may also take place under sea ice cover (Legendre et al. 1981; Strass and Nöthig 1996; Mundy et al. 2009; Arrigo et al. 2012). Sea ice and pelagic algae subsequently either transfer carbon to pelagic grazers or are rapidly exported toward the

seafloor (Tremblay et al. 1989; Michel et al. 1996; Nadaï et al. 2021).

Sea ice algae generally dominate algal export and contribute to a large proportion of particulate organic carbon (POC) fluxes over the deep basins (Gosselin et al. 1997; Zernova et al. 2000; Boetius et al. 2013; Lalande et al. 2019). By contrast, sea ice algae do not contribute significantly to algal and POC fluxes on Arctic shelves (Juul-Pedersen et al. 2010). In addition to algal cells, POC fluxes are usually composed of zooplankton fecal pellets, organic aggregates, and ice-rafted particulate matter (Michel et al. 1996; Fortier et al. 2002). Importantly, zooplankton are important for the regulation of POC export through grazing on algal cells and production of fast-sinking fecal pellets, simultaneously attenuating and enhancing POC fluxes (Fortier et al. 1994). Therefore, spatial and temporal variations in algal and zooplankton production lead to large variations in the composition and magnitude of POC fluxes (Michel et al. 1996; Fortier et al. 2002). In addition to natural variability, the recent anthropogenically induced decline in sea ice and the resulting increase in incident

✉ Eun Jin Yang
ejyang@kopri.re.kr

1   Division of Ocean and Atmosphere Sciences, Korea Polar Research Institute, Incheon 21990, Republic of Korea

light recently observed in the Arctic Ocean (Serreze et al. 2007; Comiso 2012; Nicolaus et al. 2012) may modify the magnitude, timing, and duration of algal growth and the seasonal development and composition of the zooplankton community, with poorly known implications for the biological carbon pump.

As a relative large portion of algal production and POC export in the Arctic Ocean occurs after snowmelt and before ice melt, and therefore, before possible detection by satellites (Mundy et al. 2009; Arrigo et al. 2012; Lalande et al. 2019; Nadaï et al. 2021), in situ under-ice measurements are critical to accurately estimate the potential importance of POC export to the biological carbon pump during sea ice melt. In this context, the objective of the present study was to evaluate spatial variations in the magnitude and composition of POC fluxes at a high spatial resolution under sea ice. To attain this objective, a total of 25 short-term drifting sediment traps deployments were completed at two ice camp sites visited during August 2018 over the rarely sampled Chukchi Plateau, a wide ridge extending from the Chukchi Sea shelf between the Mendeleev Ridge and the Northwind Ridge in the Pacific Arctic region (Fig. 1). In addition to POC fluxes, under-ice fluxes of chlorophyll *a* (chl *a*), an indicator of algal production, were also measured, and zooplankton collected in the sediment traps were quantified and identified to estimate the impact of grazing on under-ice fluxes. Overall, these measurements provide insights into the biological properties influencing the spatial variability of the magnitude of under-ice production and export in a rapidly changing but relatively little studied region of the Arctic Ocean.

2 Materials and Methods

2.1 Study Sites

Ice camps were set up on two drifting first-year ice floes with extensive melt ponds visited at the northernmost sites reached over the Chukchi Plateau (CP) during the ARA09B expedition on board the Korean IBRV *Araon* to the Pacific Arctic region in August 2018 (Fig. 1). The first ice floe (CP1) visited from August 17 to 19 consisted of a mix of flat and distorted first-year ice covered by a thin snow layer and refrozen meltponds (Veyssière et al. 2022). The second ice floe (CP2) visited from August 20 to 22 was also composed of first-year ice covered by refrozen meltponds (Veyssière et al. 2022). While a thin, melting snow cover was observed at both sites, the CP1 ice floe was overall thicker (0.70–1.25 m) than the CP2 ice floe (0.40–0.88 m; Veyssière et al. 2022). Images obtained from the under-ice deployment of a remotely operated vehicle showed sea ice algae filaments at both sites (Fig. 2).

2.2 CTD-Rosette Measurements

Vertical profiles of water temperature, salinity, and fluorescence-derived chlorophyll were obtained at the stations sampled immediately after the completion of each ice camp through SBE 911plus CTD casts (Sea-Bird Scientific, USA) equipped with a fluorescence sensor. Seawater samples collected at discrete depths in the upper 100 m using a rosette system holding 10 L Niskin bottles were analyzed for nutrients and concentrations of suspended chl *a* and
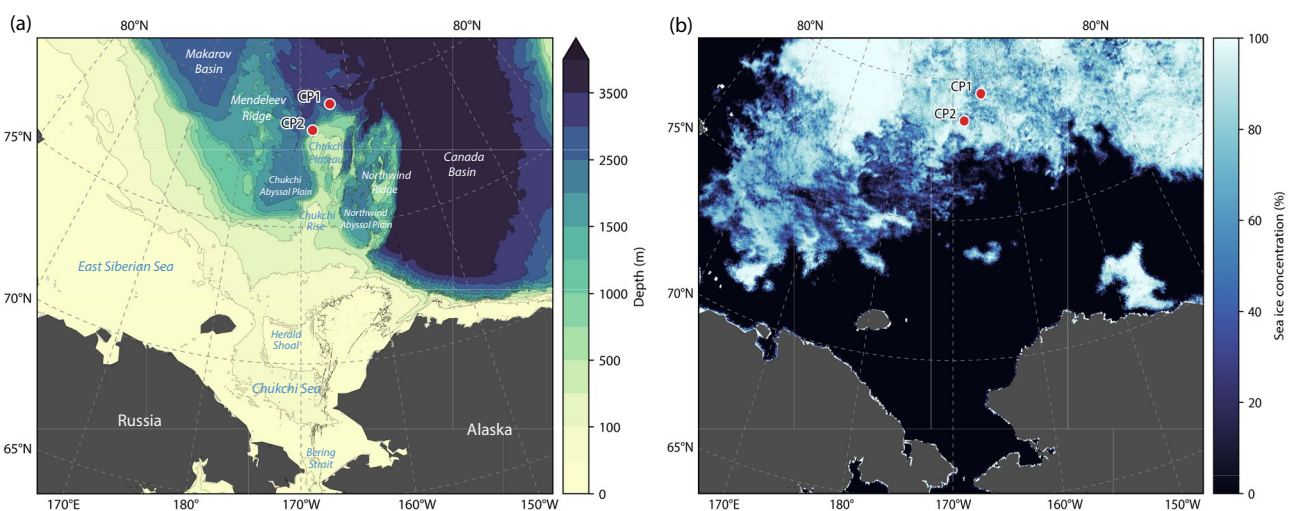
Fig. 1 a Location of the two ice camps visited over the Chukchi Plateau in the Pacific Arctic region, and **b** satellite-derived daily sea ice concentration on 19 August 2018 retrieved at a 3.125 km resolution from the AMSR2 satellite data archive of the University of Bremen (https://seaice.uni-bremen.de/data/amsr2)

Fig. 2 Sea ice algae images obtained using a digital imagery system (GoPro HERO 4) mounted on a remotely-operated vehicle deployed under ice **(a–d)** at CP1 and **(e–f)** at CP2 over the Chukchi Plateau during August 2018
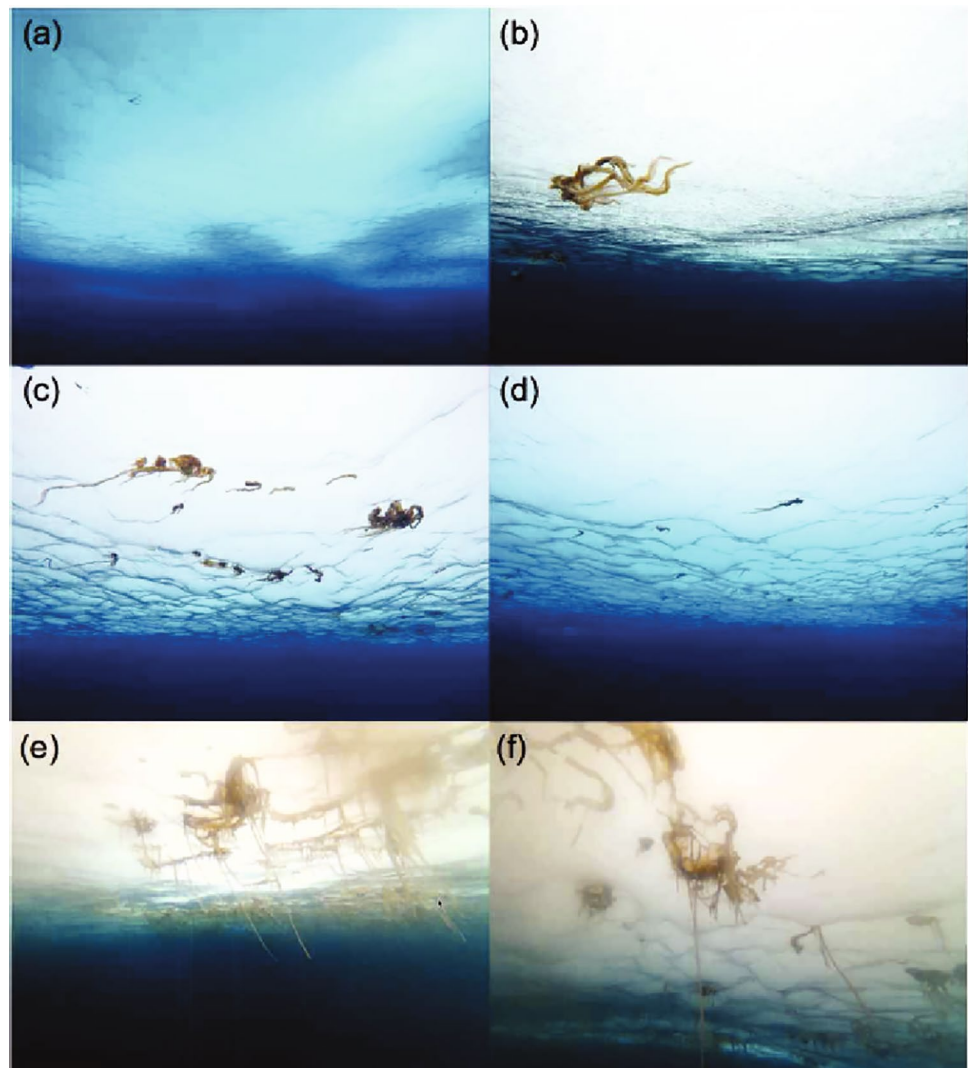
POC. Seawater samples were transferred into 50 mL conical tubes stored at 4 ℃ prior to nutrient analyses. Nitrate (NO_3^-) + nitrite (NO_2^-), silica (SiO_2), and phosphate (PO_4^{3-}) concentrations were measured using standard colorimetric methods adapted for use with a four-channel continuous auto-analyzer (QuAAtro; Seal Analytical, USA). Seawater samples for POC measurements were collected into pre-rinsed amber polyethylene bottles. Subsamples (500 mL–1 L) were then filtered onto 47 mm diameter Whatman GF/F filters pre-combusted at 550 °C for 6 h and stored at − 80 °C until laboratory analyses. Seawater subsamples (300–500 mL) were also filtered onboard through a cascade connection filtration system containing a 20 μm nylon mesh, a 2 μm Whatman Nuclepore filter, and a 0.7 μm Whatman GF/F filter to determine the chl a concentration of microphytoplankton (> 20 μm), nanophytoplankton (2–20 μm), and picophytoplankton (< 2 μm) following Sieburth et al. (1978). Each filter was extracted in 90% acetone in the dark for 12 to 24 h before fluorescence was measured using a

pre-calibrated Trilogy Turner Designs fluorometer to determine chl a concentrations following Parsons et al. (1984). The relation between total chl a concentrations obtained from seawater subsamples and fluorescence-derived chl a values obtained at the same depths was used to adjust the offset in CTD-derived fluorescence measurements.

2.3 Sediment Trap Deployments

Short-term sediment traps deployed at CP1 and CP2 consisted of cylindrical tubes (2.1 or 3.5 L) with height:diameter ratios larger than 8 to reduce turbulent mixing (Knauer and Asper 1989). A total of 25 sediment traps were deployed under ice or in open water at depths ranging from 5 to 30 m at CP1, and at depths ranging from 2 to 10 m at CP2 (Fig. 1; Table 1). Each sediment trap was attached to a single line and deployed in individual ice holes made with an auger at distances ranging from 1 to 18 m from each other for periods ranging from 30 to 54.5 h (Table 1). At CP2, three sediment

Table 1 Short-term sediment trap deployment information, with asterisks indicating open water sediment trap deployments

Ice camp	Latitude (°N)	Longitude (°W)	Deployment date	Recovery date	Water depth (m)	Trap depth (m)	Sampling period (h)
CP1	79°12.869	164°08.760	17 Aug 2018	19 Aug 2018	1903	5, 10, 30	51–54.5
CP2	78°21.655	167°47.389	20 Aug 2018	22 Aug 2018	556	2, 5*, 10	30–33, 36.5*

traps were also attached on three distinct lines anchored to the *Araon* approximately 5 m away from the ice floe edge and deployed in open water at 5 m depth for 36.5 h (Table 1). All sediment traps were weighted to remain vertical in the water column and filled with a solution of filtered seawater, formalin, and borate to preserve samples. Upon recovery, sediment trap samples were transferred into plastic bags and stored at 4 °C. Prior to subsampling, recognizable zooplankton were removed with forceps from samples obtained at 2, 5, and 10 m and preserved in a formalin solution. Subsamples for POC and particulate nitrogen (PN) measurements (1.2–2 L) were filtered onto 47 mm Whatman GF/F filters pre-combusted at 550 °C for 6 h and stored at 80 °C until laboratory analyses. Subsamples (300 mL) were filtered onto Whatman GF/F filters and extracted in 90% acetone for 24 h in the dark prior to fluorescence measurement using the same pre-calibrated Trilogy Turner Designs fluorometer used for CTD-derived measurements.

2.4 Laboratory Analyses

Zooplankton previously removed from the sediment trap samples were enumerated and identified to the lowest taxonomic level possible using a microscope. Filters for POC and PN measurements were freeze-dried before being exposed to hydrochloric acid (HCl) fumes during 24 h to remove inorganic carbon prior to measurements on a CHN elemental analyzer (vario Macro cube, Elementar, Germany). Acetanilide was used as a standard and the precision of these measurements was $\pm 4\%$ (Jung et al. 2020).

Student's *t*-tests were used to evaluate the difference in POC and chl *a* fluxes between ice camp sites.

3 Results

3.1 Water Column Properties

Low water temperature (< -1.2°C) and low salinity (< 29) were recorded in the upper water column above a thermocline and halocline measured at 40–45 m at CP1 and at 28–38 m at CP2 (Fig. 3a and b). Peaks in fluorescence-derived chlorophyll concentrations (> 0.6 mg m^{-3}) were also observed at the pycnocline depths at CP1 and CP2 (Fig. 3c). Nutrients were depleted or had very low concentrations above the pycnocline at both sites (Fig. 3d–f). Suspended POC concentration profiles were similar at both sites, with peak POC concentration values > 0.5 µmol L^{-1} observed at 47 m at CP1 and at 36 m at CP2 (Fig. 3g).

Peaks in suspended chl *a* concentrations (> 0.5 µg L^{-1}) were observed at 44 m at CP1 and at 34 m at CP2, similar to the fluorescence measurements (Fig. 4). The relative proportion of microphytoplankton (> 20 µm) in the total chl *a* concentrations remained below 25% and gradually decreased from the surface to the subsurface chl *a* maximum (SCM) depth at both sites. More than 50% of the chl *a* measured at the SCM depth was attributed to picophytoplankton (< 2 µm) at both sites (Fig. 4).
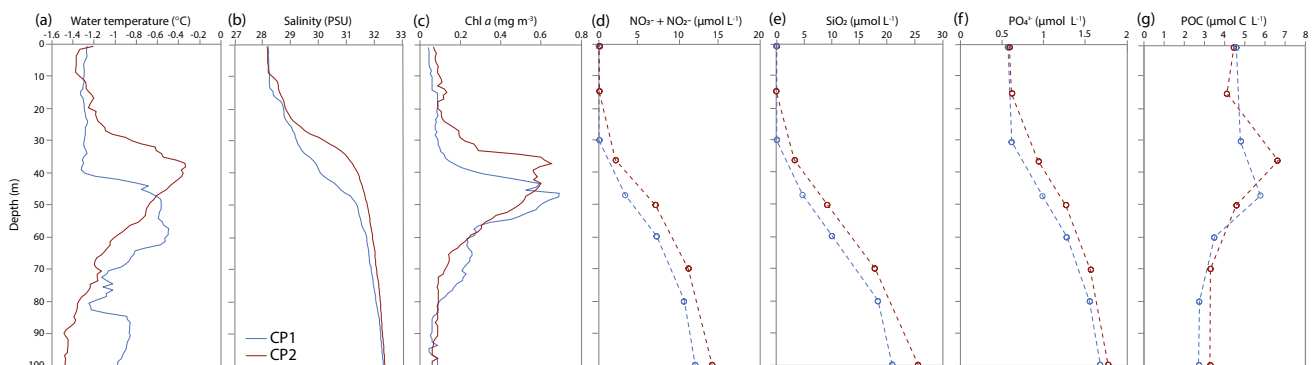
Fig. 3 **a** Water temperature, **b** salinity, and suspended concentrations of **(c)** fluorescence-derived chlorophyll, **d** nitrate (NO$_3^-$) + nitrite (NO$_2^-$), **e** silica (SiO$_2$), **f** phosphate (PO$_4^{3-}$) and **g** particulate organic carbon (POC) obtained at the completion of two ice camps over the Chukchi Plateau during August 2018. Dotted lines in **(c–f)** are used to fill gaps between the discrete data

Fig. 4 Suspended chlorophyll *a* (chl *a*) concentrations and relative contribution of size-fractionated chl *a* concentrations obtained at the completion of two ice camps over the Chukchi Plateau during August 2018. Dotted lines are used to fill gaps between the discrete data
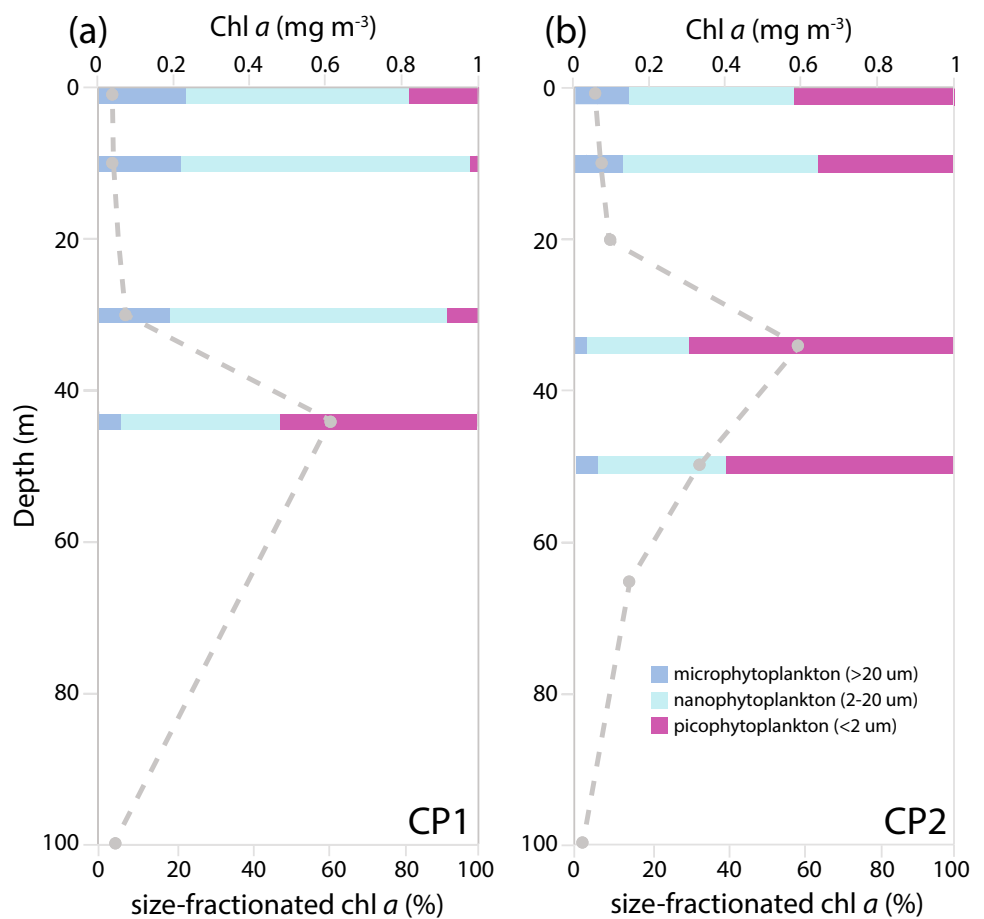
3.2 Export Fluxes

Under-ice POC fluxes were the lowest at 30 m at CP1 (208 mg m^{-2} d^{-1}) and the highest at 5 m at CP2 (1604 mg m^{-2} d^{-1}; Fig. 5a). Except for the lowest POC fluxes

recorded at one of the CP2 open water sites (259 mg m^{-2} d^{-1}), POC fluxes at 5 m were higher at CP2 (838–1604 mg C m^{-2} d^{-1}) than at CP1 (421–780 mg C m^{-2} d^{-1}; $p < 0.05$). By contrast, under-ice POC fluxes at 10 m were lower at CP2 (269–527 mg m^{-2} d^{-1}) than at CP1 (629–772 mg m^{-2}
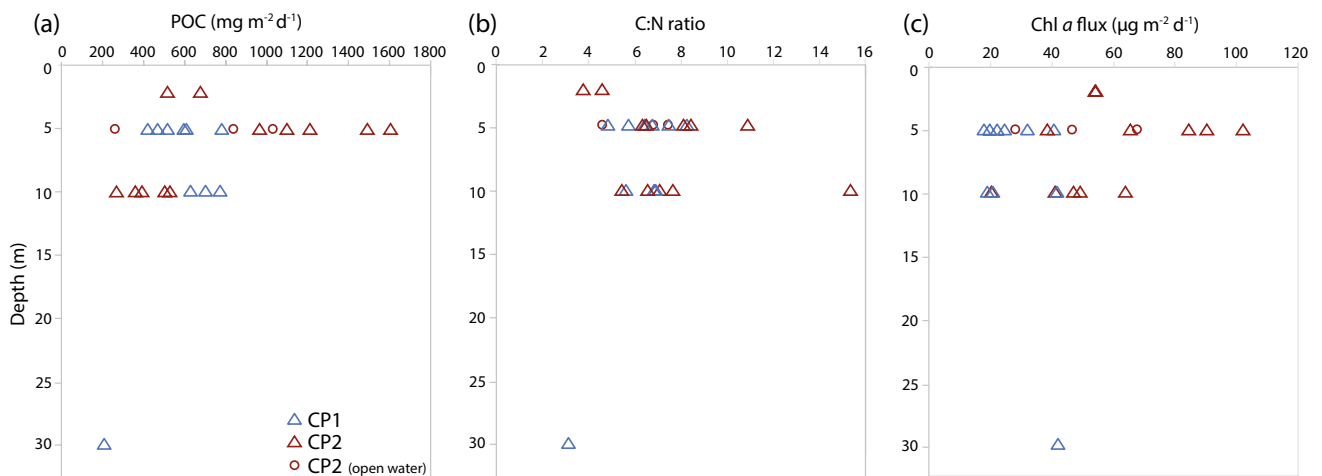
Fig. 5 Under-ice **(a)** particulate organic carbon (POC) flux, **b** C:N ratios of the sinking particles, and **c** chlorophyll *a* (chl *a*) flux obtained at two ice camps over the Chukchi Plateau during August 2018

d^{-1}; $p < 0.05$). The *C:N* ratio of the sinking particles was the lowest at 30 m at CP1 (3.1) and the highest at 10 m at CP2 (15.2; Fig. 5b). At CP1, *C:N* ratio values displayed larger variations at 5 m (4.8–8.2) than at 10 m (5.5–6.8), while at CP2, the largest variations in *C:N* ratio values were recorded at 10 m (5.4–15.3). Similar to POC fluxes, chl *a* fluxes at 5 m were higher at CP2 (28–102 µg m^{-2} d^{-1}) than at CP1 (17–40 µg m^{-2} d^{-1}; $p < 0.05$; Fig. 5c). Contrary to POC fluxes, chl *a* fluxes obtained at 10 m at CP1

(19–41 µg m^{-2} d^{-1}) and CP2 (20–63 µg m^{-2} d^{-1}) were not statistically different.

3.3 Zooplankton

Nearly all the zooplankton collected in the sediment traps were copepods (Fig. 6). The average number of copepods collected at CP1 at 10 m was at least 5 times higher than the average numbers of copepods collected at CP1 at 5 m and at

Fig. 6 Zooplankton and relative abundance of zooplankton collected in the sediment traps at two ice camps over the Chukchi Plateau during August 2018
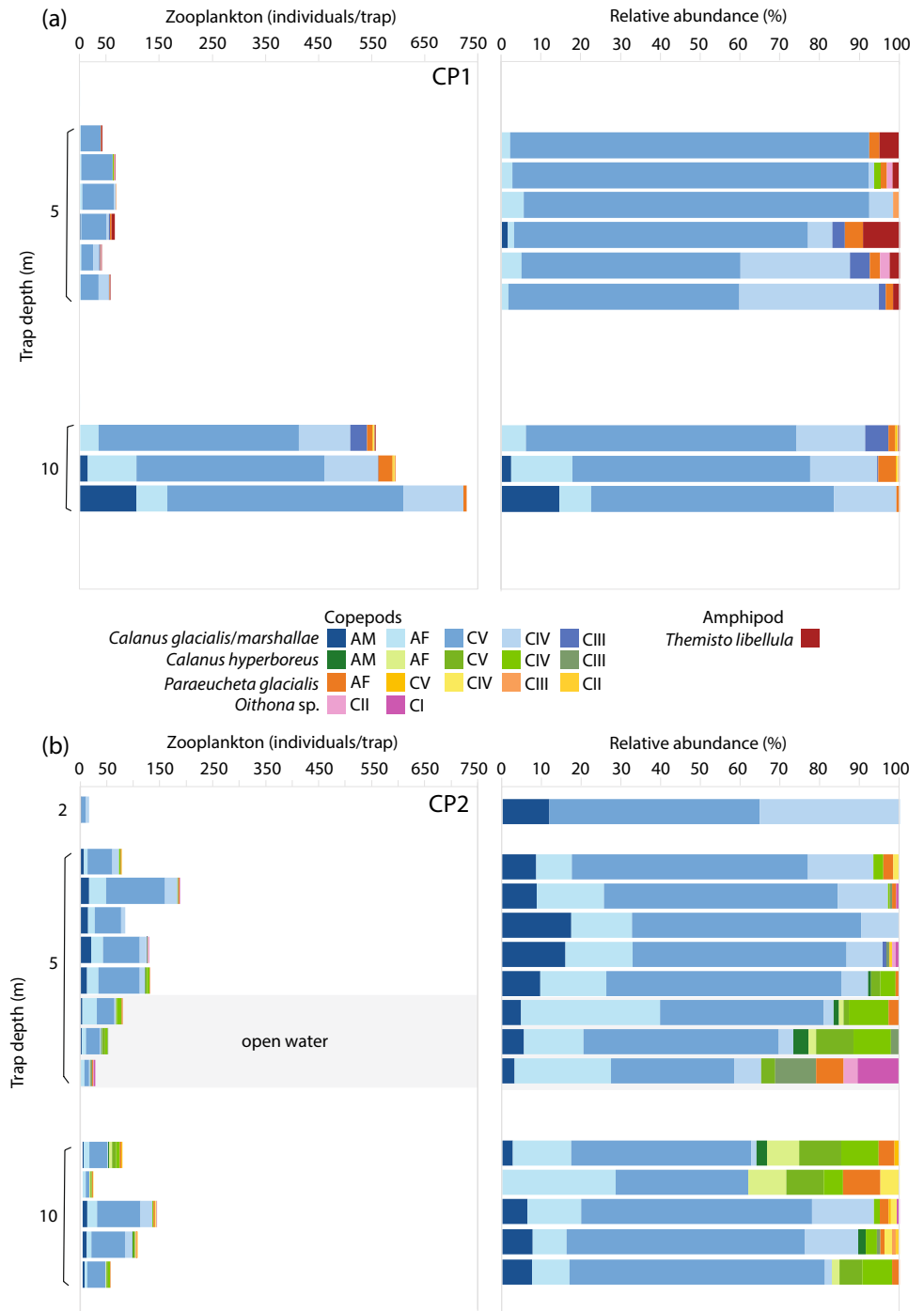
all depths sampled at CP2. In all sediment traps, the majority of copepods collected consisted of the copepod *Calanus glacialis/marshallae* (Fig. 6). As juveniles (copepodite stages) and adults of the Arctic *C. glacialis* and the Pacific *C. marshallae* are difficult to differentiate, these individuals were combined and identified as *C. glacialis/marshallae* (Hopcroft et al. 2010; Questel et al. 2013; Ashjian et al. 2017). Among the *C. glacialis/marshallae* copepods, individuals of the copepodite stage CIV were dominant at both sites and at all depths sampled (Fig. 6). The other zooplankton collected at CP1 consisted of the copepods *Paraeucheta glacialis* and *Oithona similis*, and the amphipod *Themisto libellula*. At CP2, the other zooplankton collected at 5 and 10 m mostly consisted of the copepods *Calanus hyperboreus* and *P. glacialis* (Fig. 6).

4　Discussion

4.1　Export Fluxes Associated with Sea Ice Algae Release

Sea ice properties at the CP1 and CP2 first-year ice floes displayed low salinity, low chl *a* concentrations, and very low nutrient concentrations, indicating that both ice floes were nutrient-limited and in advanced stages of melting and algal growth (Veyssière et al. 2022). Accordingly, the fresh and cold surface water layer, the nearly depleted nutrients, and the low suspended chl *a* and POC concentrations observed in the upper water column at CP1 and CP2 further reflected ongoing ice melt and indicated post-bloom conditions at both ice camps. Despite post-bloom conditions, high chl *a* and POC fluxes and low *C:N* ratios of the sinking particles collected at 5 m under both ice floes suggested the export of freshly produced material, such as sea ice algae. Although sediment trap samples were not microscopically examined to confirm and quantify the export of sea ice algae, the observation of large algal aggregates (Fig. 2) may have led to the relatively high chl *a* and POC fluxes recorded at both sites. Moreover, a greater abundance of sea ice algae filaments observed underneath the ice at CP2, where chl *a* and POC fluxes were on average twice larger than at CP1, supported sea ice algae strands as an important source of chl *a* and POC at that site. Such algal strands are typically composed of the exclusively sympagic centric diatom *Melosira arctica* that forms long brownish filaments commonly observed attached to the underside of the ice, as free-floating filaments in the meltwater layer, or as deposited aggregates on the seafloor of the deep central basins (e.g.,Gran 1899; Booth and Horner 1997; Lee et al. 2011; Boetius et al. 2013). Whereas sea ice algae export typically begins at the onset of snowmelt during spring (Nadaï et al. 2021), a delay in the export of *M. arctica* has previously been observed over the Lomonosov

Ridge, East Siberian Sea, and over the deep Nansen and Amundsen basins (Lalande et al. 2019). This delay in export may result from the formation of gas bubbles produced by photosynthetic oxygen production within the mucous matrix, regulating the buoyancy of the *M. arctica* aggregates even at low ambient nutrient concentrations (Fernández-Méndez et al. 2014). The distinct properties of this widespread sea ice algae make it a likely source of chl *a* and POC later in the productive season. Therefore, we hypothesize that the patchy under-ice distribution of the apparent *M. arctica* aggregates led to the spatial variations in chl *a* and POC fluxes observed at CP1 and CP2. Furthermore, the lower chl *a* and POC flux values observed in open water than under-ice at CP2 suggest a reduced collection of *M. arctica* due to a lower density of the sea ice algae in open water compared to under ice.

Small algal cells (nano-sized chl *a*; 2–20 μm) dominated the low suspended chl *a* concentrations at both ice camp sites during summer, similar to previous observations in the Pacific Arctic region and in the Central Arctic Ocean (Booth and Horner 1997; Gosselin et al. 1997; Lee et al. 2019). However, small algal cells, such as flagellates, dinoflagellates, and silicoflagellates, typically only contribute to a low fraction of the algal fluxes. Instead, diatoms (micro-sized chl *a*; > 20 μm) consistently dominate algal flux in the Arctic Ocean due to their high sinking rates associated with their heavy silicate frustules and formation of aggregates (Lalande et al. 2019; Dezutter et al. 2021; Nadaï et al. 2021), supporting a similar dominance of diatoms, presumably *M. arctica*, in chl *a* fluxes at CP1 and CP2.

4.2　Export Fluxes Associated with Particulate Matter Release

Alternatively, the higher POC fluxes observed at 5 m under a thinner sea ice cover at CP2 may also reflect an enhanced release of particulate matter from the melting ice at that site. Indeed, a substantial amount of resuspended particulate matter is commonly incorporated into sea ice during the freezing period over the shallow shelves and transported over the basins (Eicken et al. 2000; Eicken 2004; Wegner et al. 2005; Lalande et al. 2014). Exceptionally high concentrations of particulate matter have previously been observed into first-year sea ice over the broad Siberian shelves (Eicken et al. 2000), and high sediment loads may also be widespread in the Chukchi Sea (Eicken 2004). As sediment-laden ice displays a patchy distribution as it drifts toward the basin (Eicken et al. 2000; Eicken 2004), the higher under-ice POC fluxes observed at CP2 may reflect a larger release of POC during sea ice melt at that site. Although the contribution of the released POC to the under-ice POC fluxes has not been quantified, it should not be ignored as a potentially significant source of POC in this region.

4.3 Impact of Grazing Pressure on Export Fluxes

Compared to fluxes at 5 m, averaged chl *a* and POC fluxes obtained at 10 m were slightly higher at CP1 and lower at CP2. This discrepancy between both sites may be due to the varying grazing pressure exerted by the copepod *C. glacialis/marshallae,* dominant at both sites but more abundant at CP1 at 10 m. Indeed, higher POC fluxes at CP1 at 10 m than at 5 m may indicate an enhanced export of fecal pellets due to a larger grazing pressure resulting from the much larger presence of *C. glacialis/marshallae* at that site and depth. Conversely, lower POC fluxes at 10 m than at 5 m at CP2 possibly reflected reduced fecal pellet carbon export due to a lower grazing pressure at that site. In the Arctic Ocean, *C. glacialis* feeds on ice algae to reproduce and grow (Daase et al. 2013). Specifically, *C. glacialis* adult females (AF) migrate toward the surface before or at the onset of sea ice algae production to feed underneath the ice (Søreide et al. 2010). Several weeks later, *C. glacialis* copepodite stage CIV dominates and forms the overwintering population (Søreide et al. 2010; Daase et al. 2013). Interestingly, *C. glacialis* can rapidly develop from CIV to AF under favorable conditions, even potentially spawn late in the season (Wold et al. 2011). The larger relative proportion of *C. glacialis/marshallae* AF in the copepods collected late in the season at CP2 compared to CP1 may therefore reflect sustained food supply, potentially provided by the abundant sea ice algae observed at CP2.

Although zooplankton collected in the sediment traps do not reflect their abundances in the water column, they may reflect the composition of the zooplankton community at each trap depth. In this context, the nearly exclusive presence of *C. hyperboreus* copepodite stages CIII and older at CP2 suggests a greater exchange with the adjacent deep basin, as *C. hyperboreus* is the most abundant copepod residing in the Arctic basin (Campbell et al. 2009). Despite its low numbers, the presence of this large copepod at CP2 may have contributed to the attenuation and/or to the increase of the POC flux through grazing and the production of fecal pellets. Also, the amphipod *T. libellula*, a species associated with polar water masses that forms swarms in the upper water column (Kraft et al. 2011), was exclusively present at 5 m at CP1 and likely contributed to the enhanced POC fluxes through the production of fecal pellets. Overall, the unexplained large number of copepods collected at 10 m and the exclusive presence of *T. libellula* at 5 m highlight a high spatial heterogeneity in the distribution of copepods and amphipods in the region, likely contributing to the high spatial variability in export fluxes.

4.4 High Spatial Variability in Export Fluxes

Results obtained under the drifting ice floes CP1 and CP2 over the Chukchi Plateau showed high spatial variations in the magnitude of chl *a* and POC fluxes within small areas. The high flux variability may reflect the spatial heterogeneity in the distribution of the *M. arctica* aggregates, potentially influencing the spatial distribution of copepods and amphipods feeding on these aggregates. The heterogeneous grazing pressure exerted by zooplankton is likely to have further contributed to the spatial variability in under-ice chl *a* and POC fluxes at both CP1 and CP2.

Previous under-ice export fluxes measured using drifting sediment traps across the Arctic Ocean were mostly obtained before or at the onset of ice melt and/or below the euphotic zone. North of Svalbard, the large spatial variability in the magnitude of under-ice export fluxes observed over a relatively small area during spring was attributed to variations in the composition of the phytoplankton assemblages, the grazing pressure from large grazers, the distance to the open water, and the advection of Atlantic water (Dybwad et al. 2021). In the Canadian Arctic, chl *a* fluxes obtained between 0.5 and 25 m under ice consistently reached values > 1 mg m^{-2} d^{-1} following the release of sea ice algae during June (Michel et al. 1996; Fortier et al. 2002; Juul-Pedersen et al. 2008). Whereas chl *a* fluxes observed early in the productive season in the Canadian Arctic (> 1 mg m^{-2} d^{-1}) were much larger than chl *a* fluxes observed during summer over the Chukchi Plateau (< 0.1 mg m^{-2} d^{-1}), POC fluxes at these sites were typically lower (< 400 mg m^{-2} d^{-1}) than those obtained at CP1 and CP2 (200–1600 mg m^{-2} d^{-1}). By contrast, under-ice chl *a* fluxes measured at 2 and 5 m in the Central Arctic Ocean during late summer largely remained < 0.1 mg m^{-2} d^{-1} (Lalande et al. 2014), similar to the chl *a* fluxes at CP1 and CP2. However, the POC fluxes associated to these chl *a* fluxes were also lower in the Central Arctic Ocean than in the present study over the Chukchi Plateau (< 400 mg m^{-2} d^{-1}; Lalande et al. 2014), emphasizing the remarkably high POC fluxes measured at CP1 and CP2 in August 2018.

5 Conclusions and Implications

Under-ice export flux measurements obtained at two ice camp sites over the Chukchi Plateau in August 2018 showed wide variations in chl *a* and POC fluxes. This high spatial variability in the magnitude of under-ice export fluxes was apparently due to the heterogeneous distribution of sea ice algae aggregates, possibly associated with variation in snow and ice cover thickness, the only distinctive physical feature between both ice camp sites. Interestingly, variations in the magnitude of under-ice fluxes were larger within the

few meters sampled under a drifting ice floe than over three years at a single sample site influenced by different meteorological events and zooplankton assemblages (Fortier et al. 2002). This high spatial variability reflects the considerable patchiness of the Arctic marine ecosystem and should be considered when reporting on export fluxes. Finally, these results highlighted the potential importance of sea ice algae aggregates as a source of carbon for pelagic consumers during summer, beyond the period of maximal algal export commonly observed at the onset of snow and sea ice melt. This implies that the rapid decline in sea ice may significantly reduce this source of carbon and affect the biological carbon pump, emphasizing the necessity of monitoring carbon fluxes at a high spatial and temporal resolution in the Pacific Arctic region.

Declarations

Conflict of interest The authors have no competing interests to declare that are relevant to the content of this article.

References

Arrigo KR, Perovich DK, Pickart RS, Brown ZW, van Dijken GL, Lowry KE, Mills MM, Palmer MA, Balch WM, Bahr F, Bates NR, Benitez-Nelson C, Bowler B, Brownlee E, Ehn JK, Frey KE, Garley R, Laney SR, Lubelczyk L, Mathis J, Matsuoka A, Mitchell BG, Moore GWK, Ortega-Retuerta E, Pal S, Polashenski CM, Reynolds RA, Schieber B, Sosik HM, Stephens M, Swift JH (2012) Massive phytoplankton blooms under Arctic sea ice. Science 336(6087):1408–1408. https://doi.org/10.1126/science.1215065

Ashjian CJ, Campbell RG, Gelfman C, Alatalo P, Elliott SM (2017) Mesozooplankton abundance and distribution in association with hydrography on Hanna Shoal, NE Chukchi sea, during August 2012 and 2013. Deep-Sea Res Pt II 144:21–36. https://doi.org/10.1016/j.dsr2.2017.08.012

Boetius A, Albrecht S, Bakker K, Bienhold C, Felden J, Fernández-Méndez M, Hendricks S, Katlein C, Lalande C, Krumpen T, Nicolaus M, Peeken I, Rabe B, Rogacheva A, Rybakova E, Somavilla R, Wenzhöfer F (2013) Export of algal biomass from the melting Arctic sea ice. Science 339(6126):1430–1432. https://doi.org/10.1126/science.1231346

Booth BC, Horner RA (1997) Microalgae on the arctic ocean section, 1994: species abundance and biomas. Deep-Sea Res Pt II 44(8):1607–1622. https://doi.org/10.1016/S0967-0645(97)00057-X

Campbell RG, Sherr EB, Ashjian CJ, Plourde S, Sherr BF, Hill V, Stockwell DA (2009) Mesozooplankton prey preference and grazing impact in the western Arctic ocean. Deep-Sea Res Pt II 56(17):1274–1289. https://doi.org/10.1016/j.dsr2.2008.10.027

Campbell K, Mundy CJ, Barber DG, Gosselin M (2015) Characterizing the sea ice algae chlorophyll a–snow depth relationship over Arctic spring melt using transmitted irradiance. J Marine Syst 147:76–84. https://doi.org/10.1016/j.jmarsys.2014.01.008

Comiso JC (2012) Large decadal decline of the Arctic multiyear ice cover. J Clim 25(4):1176–1193. https://doi.org/10.1175/JCLI-D-11-00113.1

Cota GF, Legendre L, Gosselin M, Ingram RG (1991) Ecology of bottom ice algae: I. environmental controls and variability. J Marine Syst 2:257–277. https://doi.org/10.1016/0924-7963(91)90036-T

Daase M, Falk-Petersen S, Varpe Ø, Darnis G, Søreide JE, Wold A, Leu E, Berge J, Philippe B, Fortier L (2013) Timing of reproductive events in the marine copepod Calanus glacialis: a pan-Arctic perspective. Can J Fish Aquat Sci 70(6):871–884. https://doi.org/10.1139/cjfas-2012-0401

Dezutter T, Lalande C, Darnis G, Fortier L (2021) Seasonal and inter-annual variability of the queen maud Gulf ecosystem derived from sediment trap measurements. Limnol Oceanogr 66(S1):S411–S426. https://doi.org/10.1002/lno.11628

Dybwad C, Assmy P, Olsen LM, Peeken I, Nikolopoulos A, Krumpen T, Randelhoff A, Tatarek A, Wiktor JM, Reigstad M (2021) Carbon export in the seasonal sea ice zone north of Svalbard from winter to late summer. Front Mar Sci 7:525800. https://doi.org/10.3389/fmars.2020.525800

Eicken H (2004) The role of Arctic sea ice in transporting and cycling terrigenous organic matter. In: Stein R, Macdonald RW (eds) The organic carbon cycle in the Arctic Ocean. Springer, New York, pp 45–54

Eicken H, Kolatschek J, Freitag J, Lindemann F, Kassens H, Dmitrenko I (2000) A key source area and constraints on entrainment for basin-scale sediment transport by Arctic sea ice. Geophys Res Lett 27(13):1919–1922. https://doi.org/10.1029/1999GL011132

Fernández-Méndez M, Wenzhöfer F, Peeken I, Sørensen HL, Glud RN, Boetius A (2014) Composition, buoyancy regulation and fate of ice algal aggregates in the central Arctic ocean. PLoS ONE 9(9):e107452. https://doi.org/10.1371/journal.pone.0107452

Fortier L, Le Fèvre J, Legendre L (1994) Export of biogenic carbon to fish and to the deep ocean: the role of large planktonic microphages. J Plankton Res 16(7):809–839. https://doi.org/10.1093/plankt/16.7.809

Fortier M, Fortier L, Michel C, Legendre L (2002) Climatic and biological forcing of the vertical flux of biogenic particles under seasonal Arctic sea ice. Mar Ecol-Prog Ser 225:1–16

Gosselin M, Levasseur M, Wheeler PA, Horner RA, Booth BC (1997) New measurements of phytoplankton and ice algal production in the Arctic Ocean. Deep-Sea Res Pt II 44(8):1623–1644. https://doi.org/10.1016/S0967-0645(97)00054-4

Gran HH (1899) Diatomaceae from the ice-floes and plankton of the Arctic Ocean. In: Nansen F (ed) Norwegian North Polar expedition 1893–1896, scientific results. Fridtjof Nansen Fund for the Advancement of Science n.d, London, p 74

Hopcroft RR, Kosobokova KN, Pinchuk AI (2010) Zooplankton community patterns in the Chukchi sea during summer 2004. Deep-Sea Res Pt II 57(1–2):27–39. https://doi.org/10.1016/j.dsr2.2009.08.003

Jung J, Hong SB, Chen M, Hur J, Jiao L, Lee Y, Park K, Hahm D, Choi JO, Yang EJ, Park J, Kim TW, Lee S (2020) Characteristics of methanesulfonic acid, non-sea-salt sulfate and organic carbon aerosols over the Amundsen Sea. Antarctica Atmos Chem Phys 20(9):5405–5424. https://doi.org/10.5194/acp-20-5405-2020

Juul-Pedersen T, Michel C, Gosselin M, Seuthe L (2008) Seasonal changes in the sinking export of particulate material under first-year sea ice on the Mackenzie Shelf (western Canadian Arctic). Mar Ecol-Prog Ser 353:13–25. https://doi.org/10.3354/meps07165

Juul-Pedersen T, Michel C, Gosselin M (2010) Sinking export of particulate organic material from the euphotic zone in the eastern Beaufort Sea. Mar Ecol-Prog Ser 410:55–70. https://doi.org/10.3354/meps08608

Knauer G, Asper V (1989) Sediment trap technology and sampling: report of the U.S. GOFS working group on sediment trap technology and sampling. U.S. GOFS Planning Coordination Office, Falmouth, p 94

Kraft A, Bauerfeind E, Nöthig E-M (2011) Amphipod abundance in sediment trap samples at the long-term observatory HAUSGARTEN (Fram Strait, ~79°N/4°E). Variability in species community patterns. Mar Biodivers 41:353–364. https://doi.org/10.1007/s12526-010-0052-1

Lalande C, Nöthig E-M, Somavilla R, Bauerfeind E, Shevchenko V, Okolodkov Y (2014) Variability in under-ice export fluxes of biogenic matter in the Arctic ocean. Glob Biogeochem Cy 28(5):571–583. https://doi.org/10.1002/2013GB00473

Lalande C, Nöthig E-M, Fortier L (2019) Algal export in the Arctic ocean in times of global warming. Geophys Res Lett 46(11):5959–5967. https://doi.org/10.1029/2019gl083167

Lee SH, McRoy CP, Joo HM, Gradinger R, Cui X, Yun MS, Chung KH, Kang S-H, Kang C-K, Choy EJ, Son S, Carmack E, Whitledge TE (2011) Holes in progressively thinning Arctic sea ice lead to new ice algae habitat. Oceanography 24(3):302–308. https://doi.org/10.5670/oceanog.2011.81

Lee Y, Min J-O, Yang EJ, Cho K-H, Jung J, Park J, Moon JK, Kang S-H (2019) Influence of sea ice concentration on phytoplankton community structure in the Chukchi and east Siberian seas, Pacific Arctic ocean. Deep-Sea Res Pt I 147:54–64. https://doi.org/10.1016/j.dsr.2019.04.001

Legendre L, Ingram RG, Poulin M (1981) Physical control of phytoplankton production under sea ice (Manitounuk sound, Hudson bay). Can J Fish Aquat Sci 38(11):1385–1392. https://doi.org/10.1139/f81-185

Leu E, Mundy CJ, Assmy P, Campbell K, Gabrielsen TM, Gosselin M, Juul-Pedersen T, Gradinger R (2015) Arctic spring awakening — steering principles behind the phenology of vernal ice algal blooms. Prog Oceanogr 139:151–170. https://doi.org/10.1016/j.pocean.2015.07.012

Michel C, Legendre L, Ingram RG, Gosselin M, Levasseur M (1996) Carbon budget of sea-ice algae in spring: evidence of a significant transfer to zooplankton grazers. J Geophys Res-Oceans 101(C8):18345–18360. https://doi.org/10.1029/96jc00045

Mundy CJ, Gosselin M, Ehn J, Gratton Y, Rossnagel A, Barber DG, Martin J, Tremblay J-É, Palmer M, Arrigo KR, Darnis G, Fortier L, Else B, Papakyriakou T (2009) Contribution of under-ice primary production to an ice-edge upwelling phytoplankton bloom in the Canadian Beaufort sea. Geophys Res Lett 36(17):L17601. https://doi.org/10.1029/2009GL038837

Nadaï G, Nöthig E-M, Fortier L, Lalande C (2021) Early snowmelt and sea ice breakup enhance algal export in the Beaufort Sea. Prog Oceanogr 190:102479. https://doi.org/10.1016/j.pocean.2020.102479

Nicolaus M, Katlein C, Maslanik J, Hendricks S (2012) Changes in Arctic sea ice result in increasing light transmittance and absorption. Geophys Res Lett 39(24):L24501. https://doi.org/10.1029/2012GL053738

Parsons TR, Maita Y, Lalli CM (1984) A manual of chemical and biological methods for seawater analysis. Pergamon Press, New York, p 173

Questel JM, Clarke C, Hopcroft RR (2013) Seasonal and interannual variation in the planktonic communities of the northeastern Chukchi Sea during the summer and early fall. Cont Shelf Res 67:23–41. https://doi.org/10.1016/j.csr.2012.11.003

Serreze MC, Holland MM, Stroeve J (2007) Perspectives on the Arctic's shrinking sea-ice cover. Science 315(5818):1533–1536. https://doi.org/10.1126/science.1139426

Sieburth JM, Smetacek V, Lenz J (1978) Pelagic ecosystem structure: heterotrophic compartments of the plankton and their relationship to plankton size fractions 1. Limnol Oceanogr 23(6):1256–1263. https://doi.org/10.4319/lo.1978.23.6.1256

Søreide JE, Leu E, Berge J, Graeve M, Falk-Petersen S (2010) Timing of blooms, algal food quality and *Calanus glacialis* reproduction and growth in a changing Arctic. Glob Change Biol 16(11):3154–3163. https://doi.org/10.1111/j.1365-2486.2010.02175.x

Strass VH, Nöthig E-M (1996) Seasonal shifts in ice edge phytoplankton blooms in the Barents sea related to the water column stability. Polar Biol 16(6):409–422. https://doi.org/10.1007/bf02390423

Tremblay C, Runge JA, Legendre L (1989) Grazing and sedimentation of ice algae during and immediately after a bloom at the ice-water interface. Mar Ecol-Prog Ser 56:291–300

Veyssière G, Castellani G, Wilkinson J, Karcher M, Hayward A, Stroeve JC, Nicolaus M, Kim J-H, Yang E-J, Valcic L, Kauker F, Khan AL, Rogers I, Jung J (2022) Under-ice light field in the Western Arctic ocean during late summer. Front Earth Sci 9:643737. https://doi.org/10.3389/feart.2021.643737

Wegner C, Hölemann JA, Dmitrenko I, Kirillov S, Kassens H (2005) Seasonal variations in Arctic sediment dynamics—evidence from 1-year records in the Laptev Sea (Siberian Arctic). Glob Planet Change 48(1):126–140. https://doi.org/10.1016/j.gloplacha.2004.12.009

Wold A, Darnis G, Søreide JE, Leu E, Philippe B, Fortier L, Poulin M, Kattner G, Graeve M, Falk-Petersen S (2011) Life strategy and diet of Calanus glacialis during the winter–spring transition in Amundsen Gulf, south-eastern Beaufort sea. Polar Biol 34(12):1929–1946. https://doi.org/10.1007/s00300-011-1062-6

Zernova VV, Nöthig EM, Shevchenko VP (2000) Vertical microalga flux in the northern Laptev Sea (from the data collected by the yearlong sediment trap). Oceanology 40(6):801–808